銀河物理学特論 I
Galactic Astrophysics I

I-1: Morphologies of galaxies

2015/04/13

Galaxy morphology and Hubble sequence
銀河形態のハッブル系列

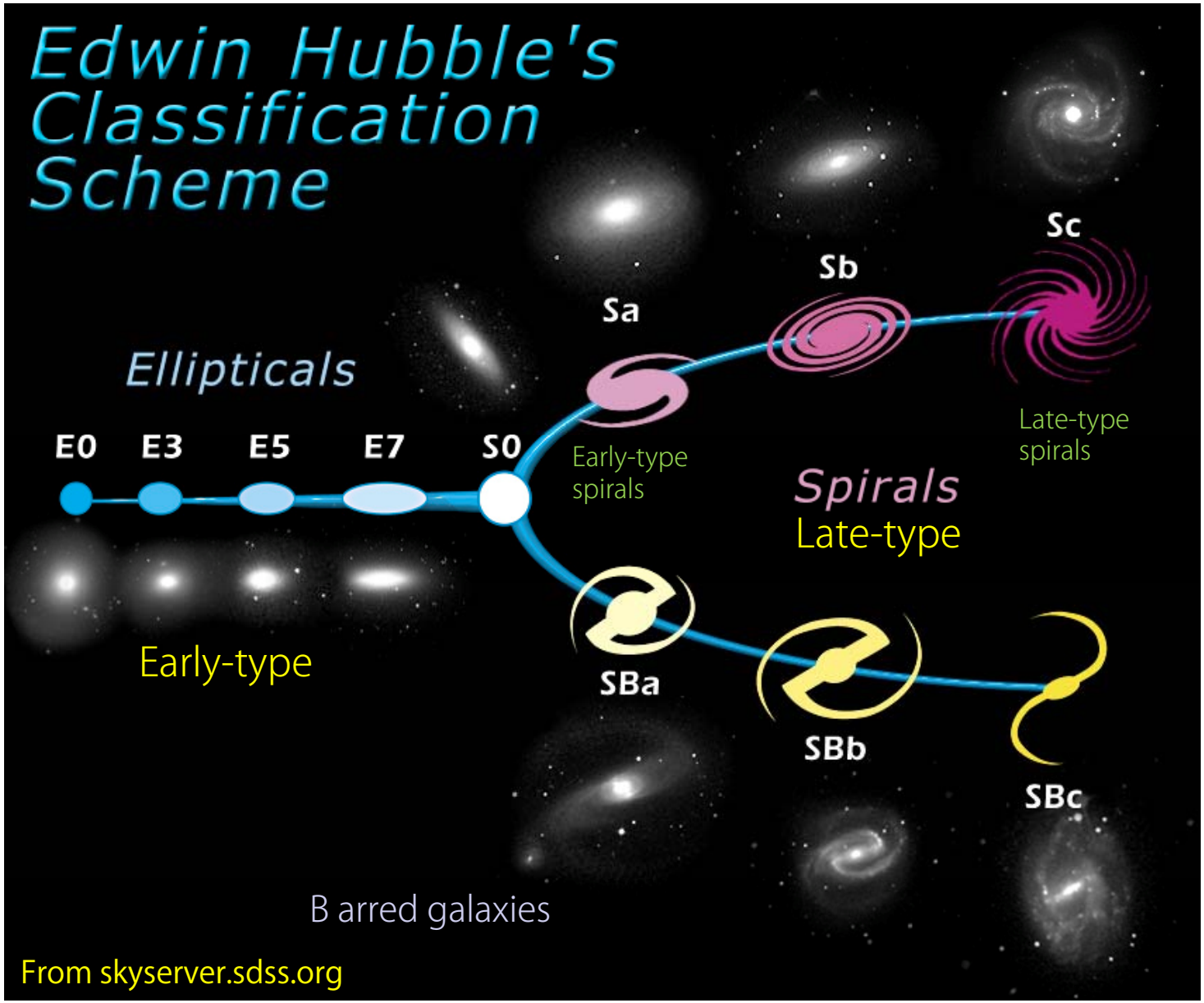

Hubble sequence
ハッブル系列

- With SDSS images. Color images made with three images taken with three different filters

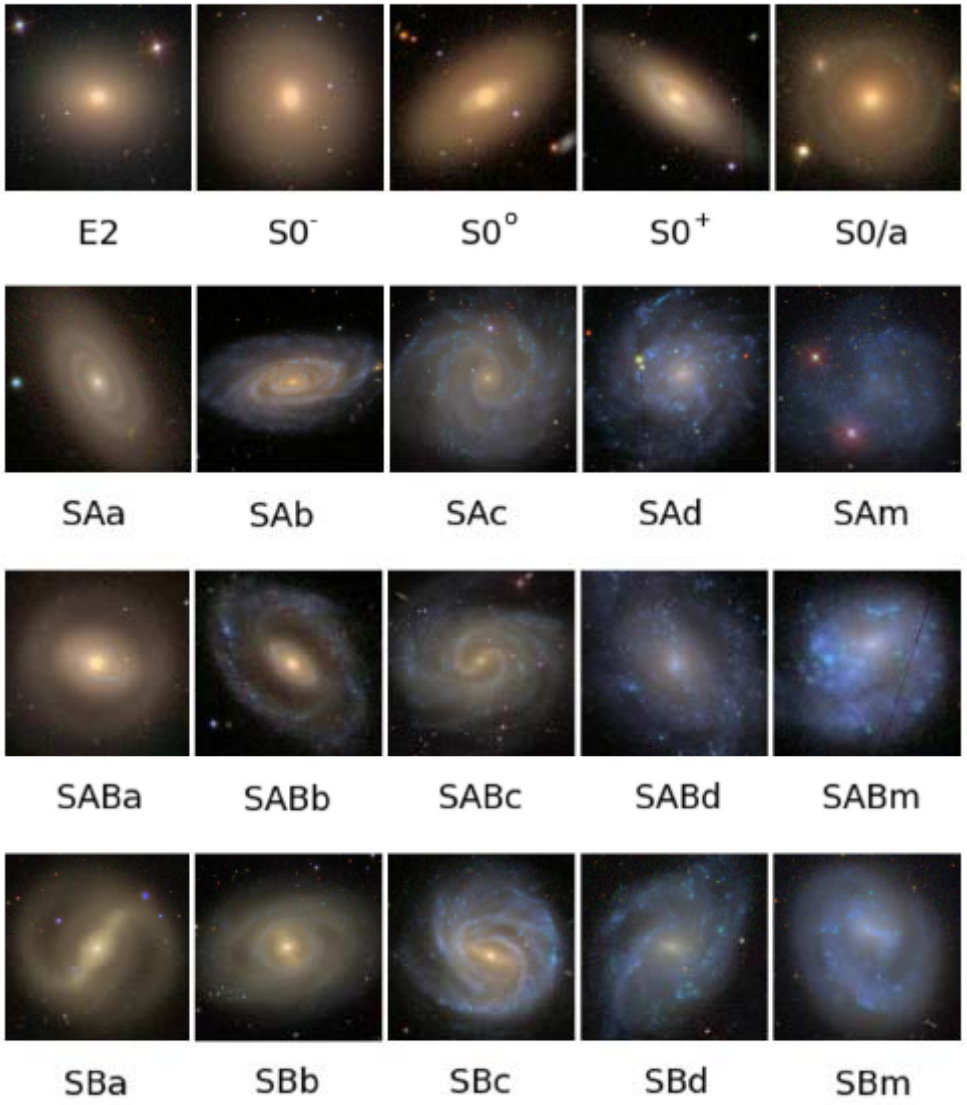

Buta, 2011, arXiv:1102.0550

Elliptical galaxies

Sloan Digital Sky Survey r<16mag sample galaxies

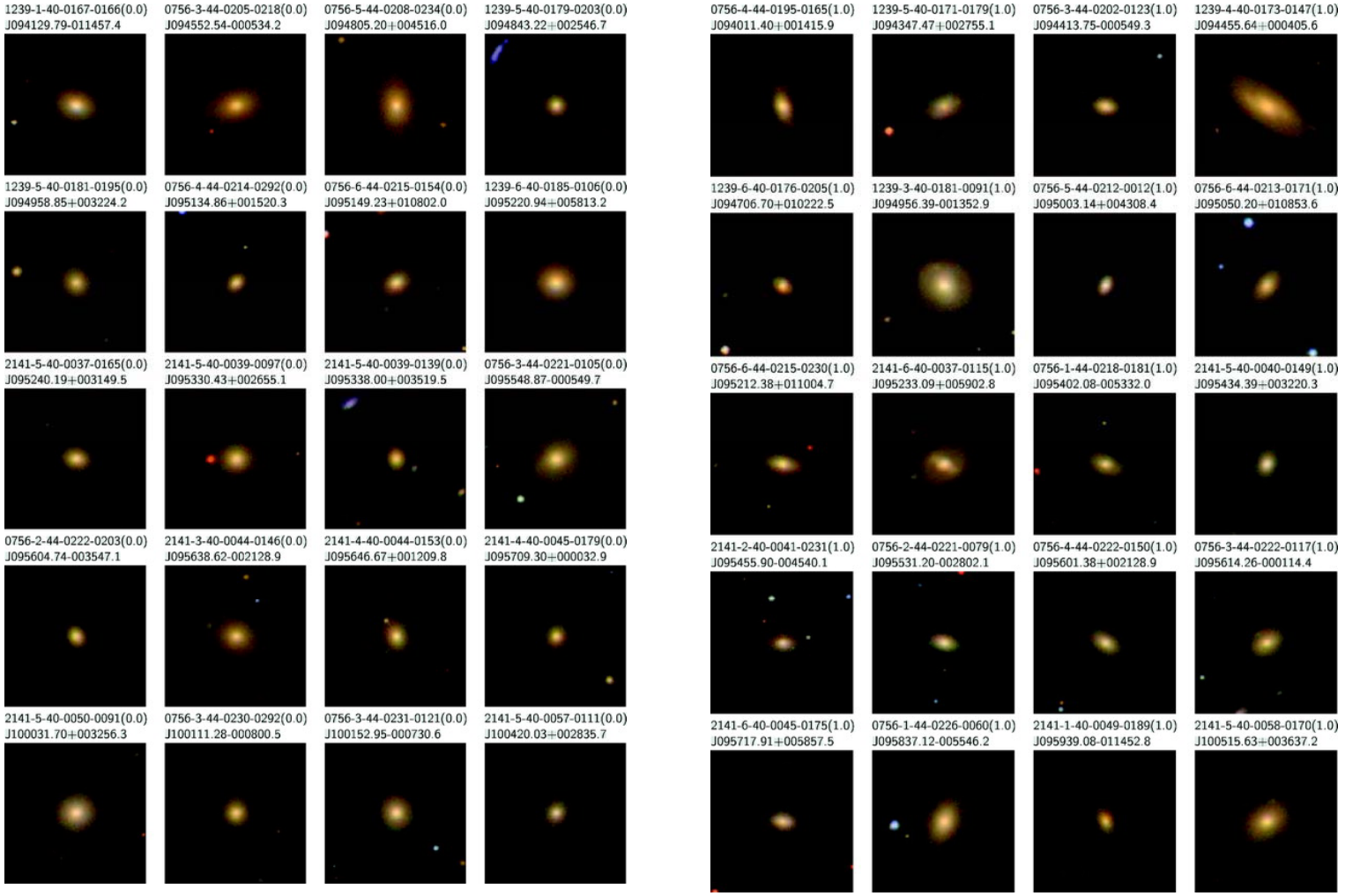

Fukugita et al. 2007, ApJ, 134, 579

Early-type spiral galaxies

Sloan Digital Sky Survey r<16mag sample galaxies

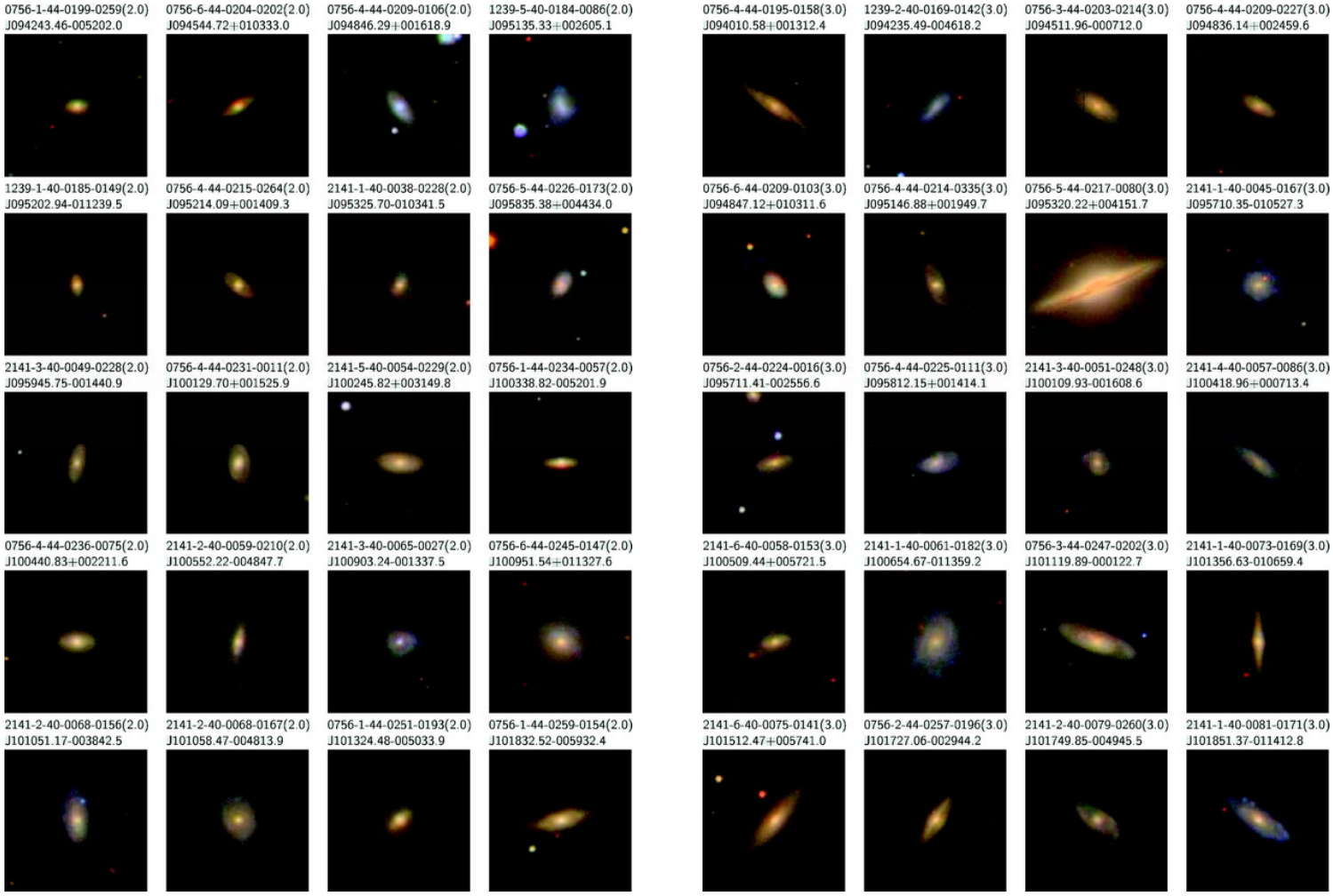

Fukugita et al. 2007, ApJ, 134, 579

Late-type Spiral galaxies Irregular galaxies

Sloan Digital Sky Survey r<16mag sample galaxies

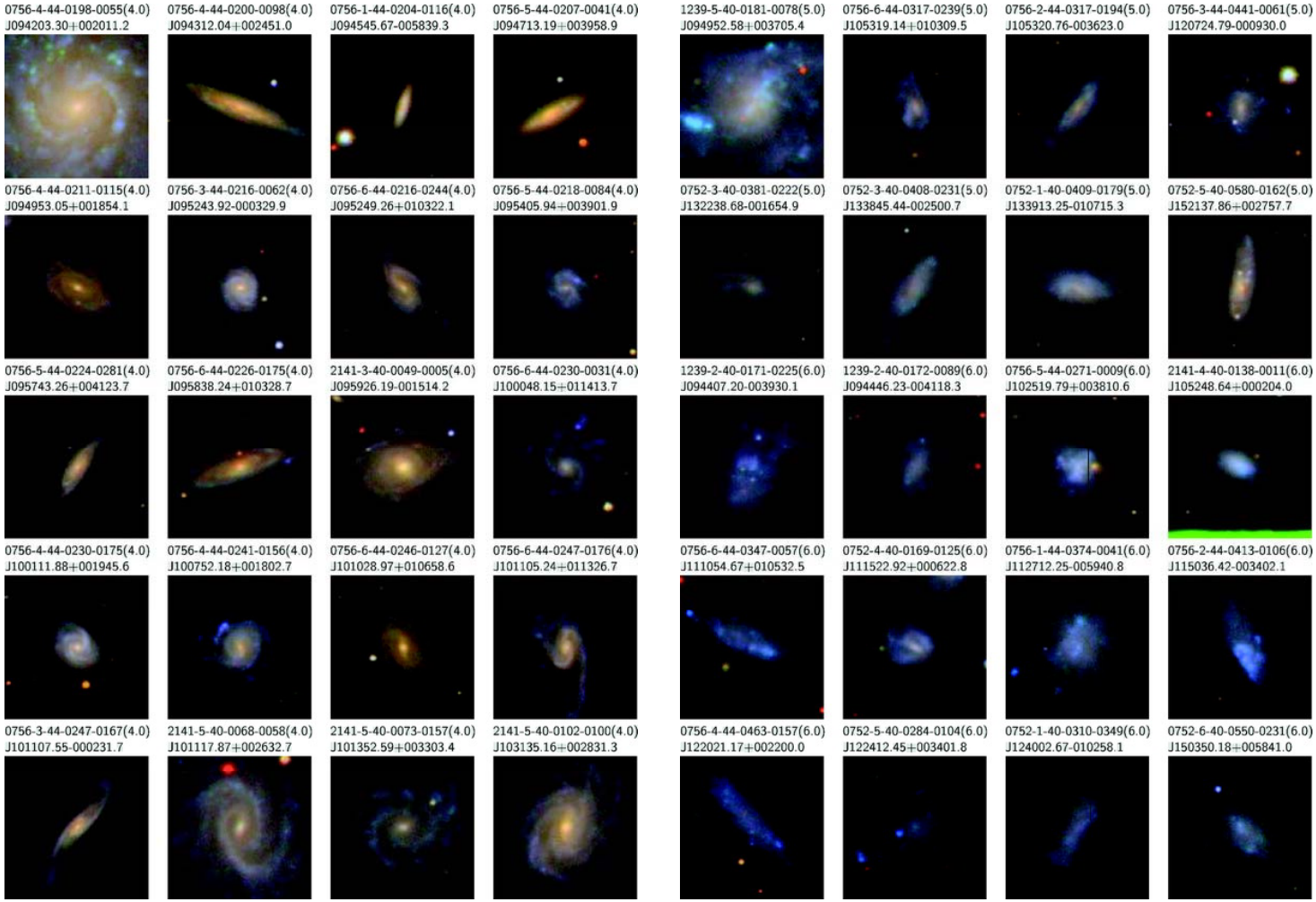

Fukugita et al. 2007, ApJ, 134, 579

Irregular galaxies, Merging galaxies

Sloan Digital Sky Survey r<16mag sample galaxies

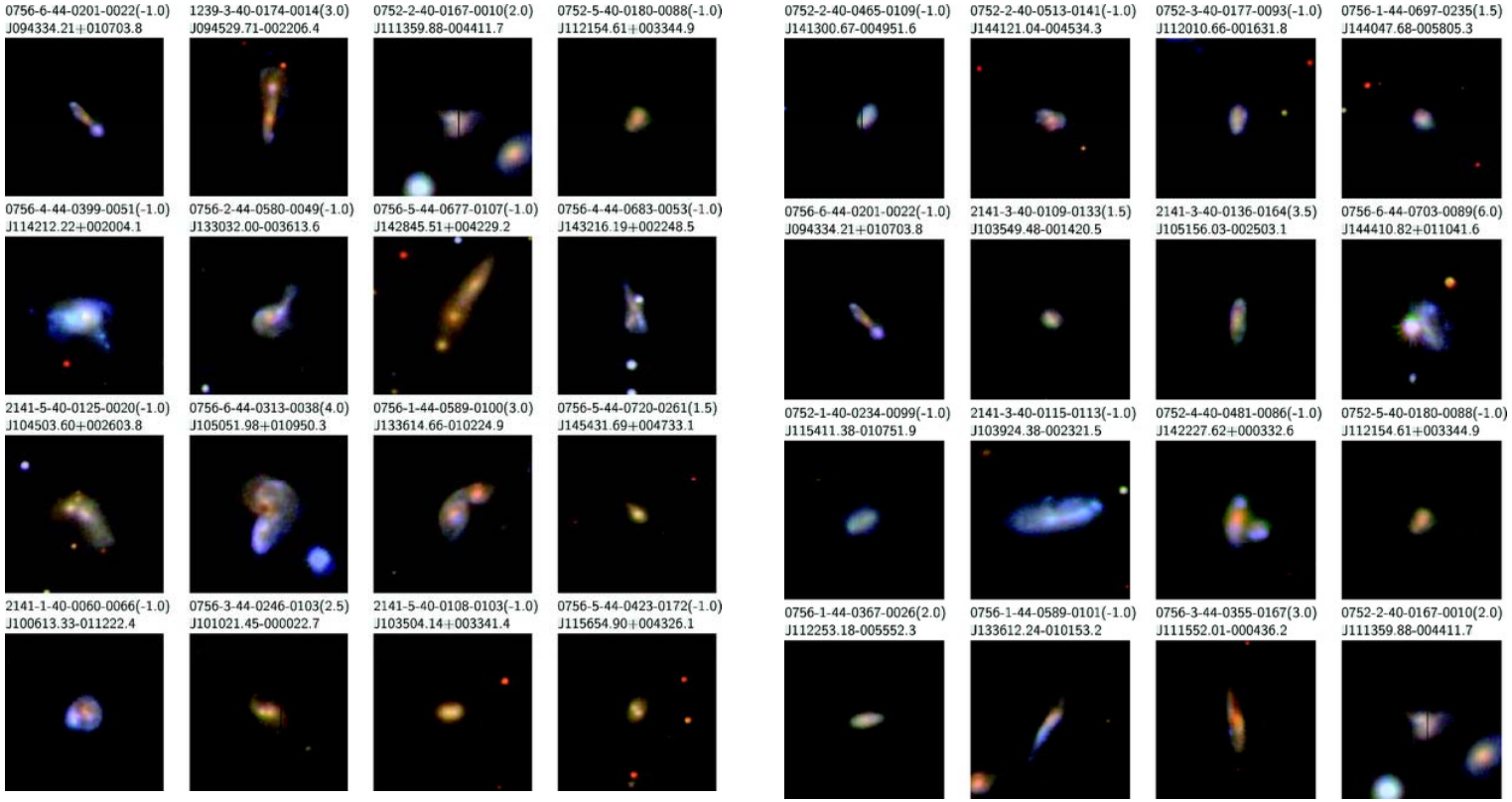

Fukugita et al. 2007, ApJ, 134, 579

Sequence of elliptical galaxies
楕円銀河の系列

- Ellipticity increases along the sequence, and goes up to E7. Elliptical galaxies larger than E7 is rare.

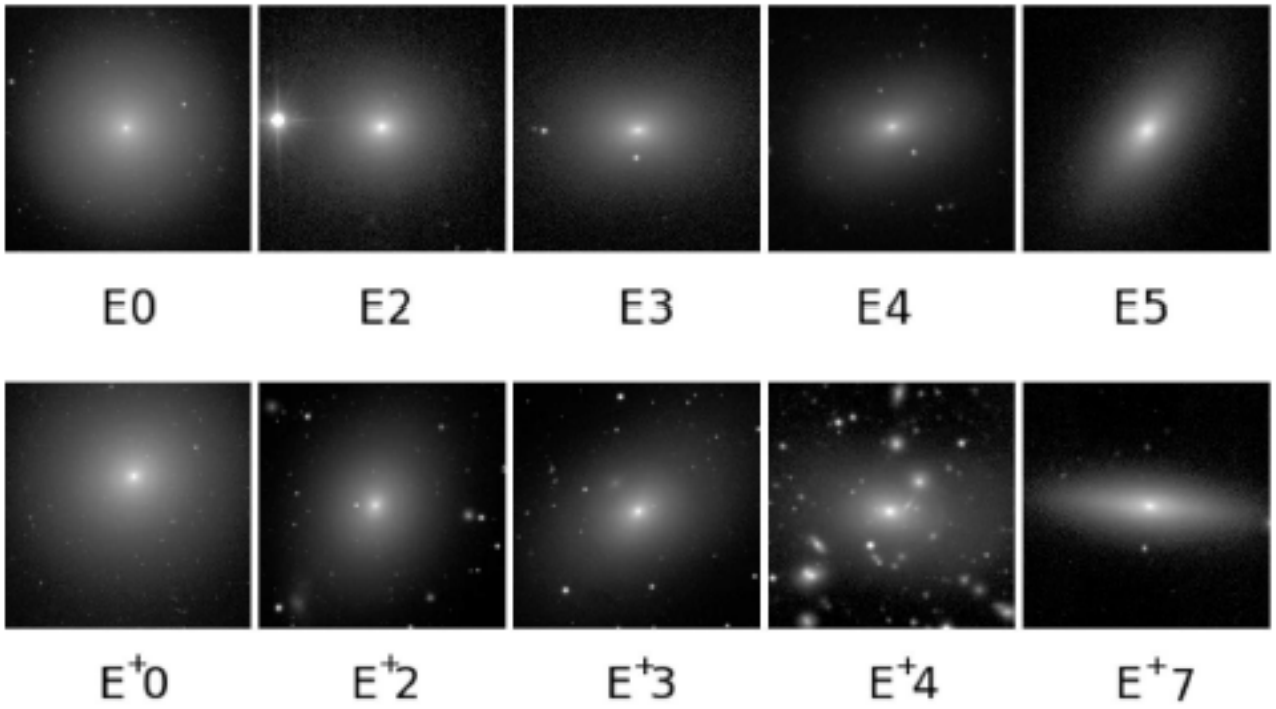

Buta, 2011, arXiv:1102.0550

Effect of viewing angle
視線の角度の影響

- Barred structure becomes difficult to be identified, ex. Milky way galaxy.

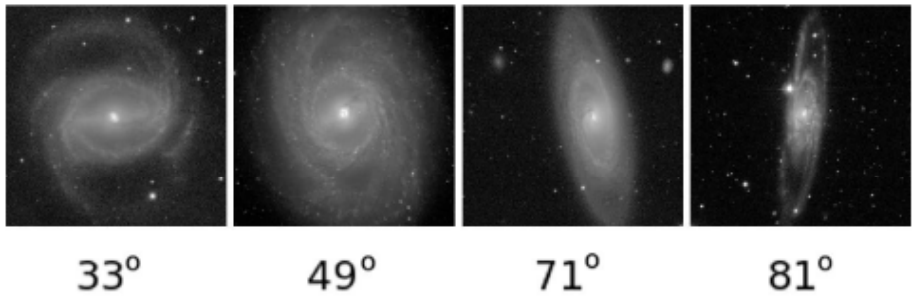

- Disk structure becomes thinner along the Hubble sequence.

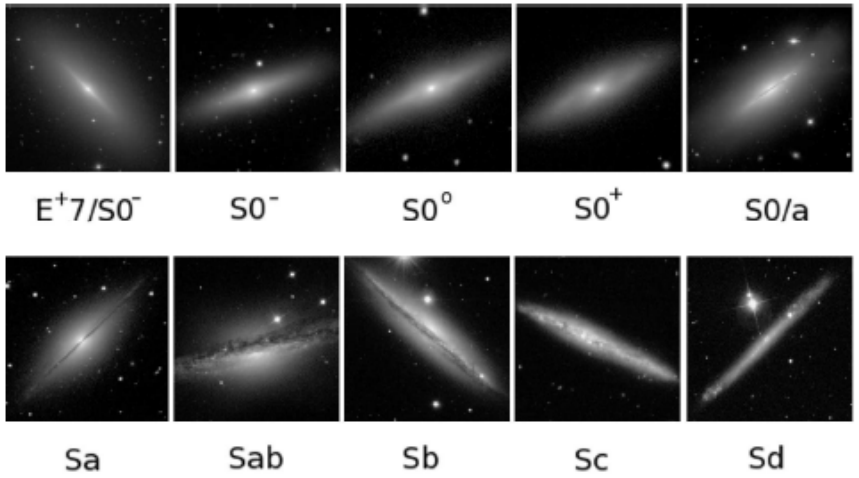

Buta, 2011, arXiv:1102.0550

Light profile
光度分布

Surface brightness:

At center

$$I_0(\mathrm{erg\ s^{-1}\ cm^{-2}\ Hz^{-1}\ arcsec^{-2}})$$
$$\mu_0(R)(\mathrm{mag\ arcsec^{-2}})$$

At effective radius

$$I_e(\mathrm{erg\ s^{-1}\ cm^{-2}\ Hz^{-1}\ arcsec^{-2}})$$
$$\mu_e(R)(\mathrm{mag\ arcsec^{-2}})$$

Radius above a certain surface brightness limit: for example 25 mag arcsec^-2

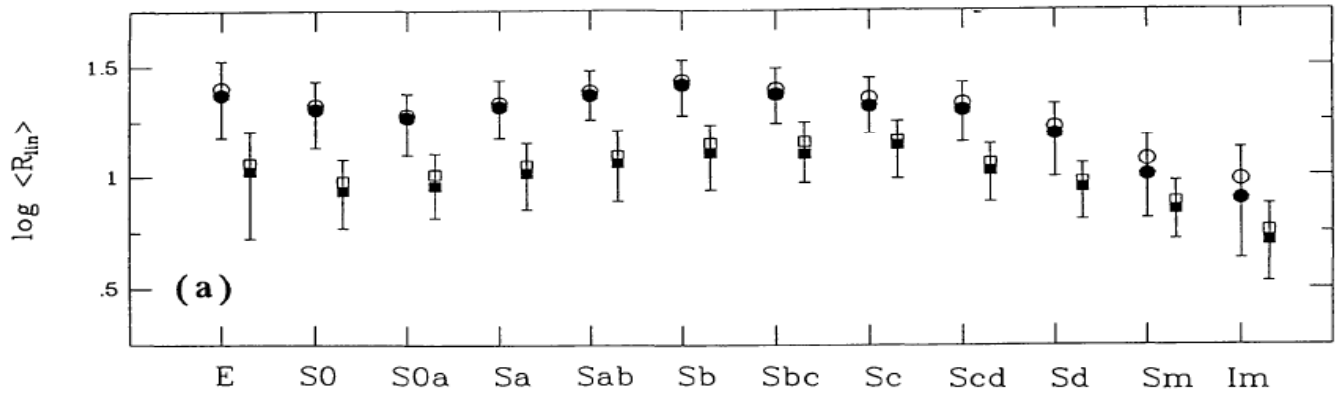

Roberts & Haynes, 1994, ARAA, 32, 115

Effective radius : within the effective radius, half of the total light of a galaxy included.

Light profile: de Vaucouleurs profile, exponential profile
光度分布：ドボークルール則、指数則

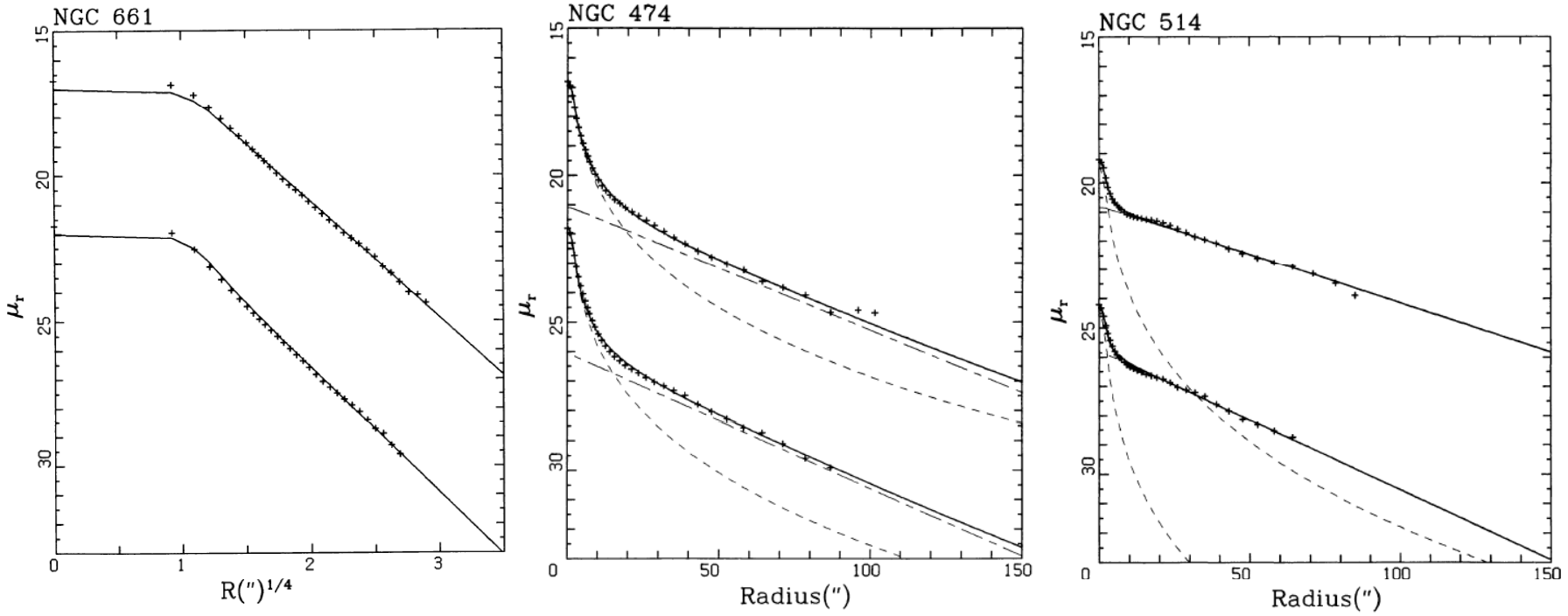

Elliptical galaxy　　Spiral galaxy

Kent 1985, ApJS, 59, 115

r1/4 profile, de Vaucouleurs profile = elliptical galaxies, bulge component of disk galaxies

$$I(R) = I_e \exp\left[-\beta_n \left[\left(\frac{R}{R_e}\right)^{1/4} - 1\right]\right]$$

Exponential profile = disk component of disk galaxies

$$I(R) = I_0 \exp\left[-\beta_n \left(\frac{R}{R_e}\right)\right]$$

Bulge-disk decomposition
バルジとディスクの分離

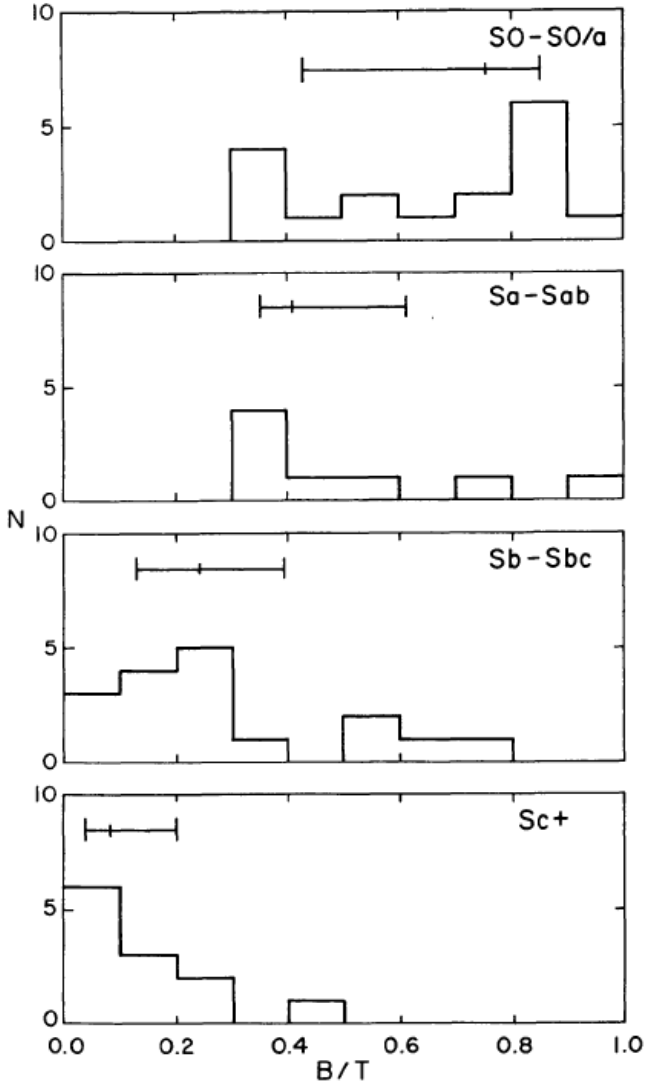

FIG. 6.—Distribution of B/T as a function of morphological type

Kent 1985, ApJS, 59, 115

Morphological Classification
形態分類

- Qualitative classification with “Asymmetry” and “Concentration”

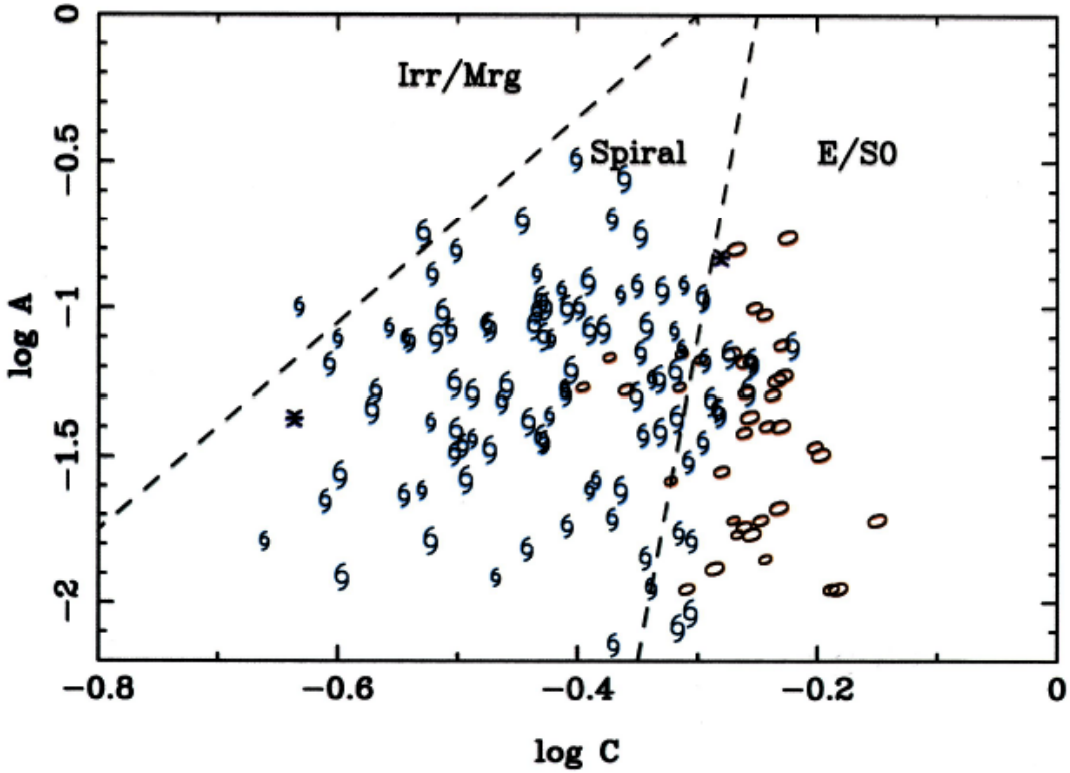

FIG. 2.—The distribution on the *C-A* plane of artificially redshifted galaxies from the Frei sample. Only objects with $I < 22$ are shown. Plot symbols denote E/S0 systems (*red ellipses*), spirals (*light blue spiral symbols*), and irregulars (*dark blue asterisks*). The sizes of the plot symbols are inversely proportional to the artificial redshifts of the galaxies (which can be one of $z = 0.3, 0.5$, or 0.7). Dashed lines delineate the three morphological bins adopted in the present work.

Abraham et al. 1996, ApJS, 107, 1

Sersic profile
セルシック則

$$I(R) = I_0 \exp\left[-\beta_n \left(\frac{R}{R_e}\right)^{1/n}\right] = I_e \exp\left[-\beta_n \left[\left(\frac{R}{R_e}\right)^{1/n} - 1\right]\right]$$

Describe the exponential and r1/4 profiles as one parameter family.

With n=1 exponential profile = disk galaxies

With n=4 r1/4 profile, de Vaucouleurs profile = elliptical galaxies

Beta is determined so that half of a galaxy light is included within its effective radius. Beta is well approximated by

$$\beta_n = 2n - 0.324$$

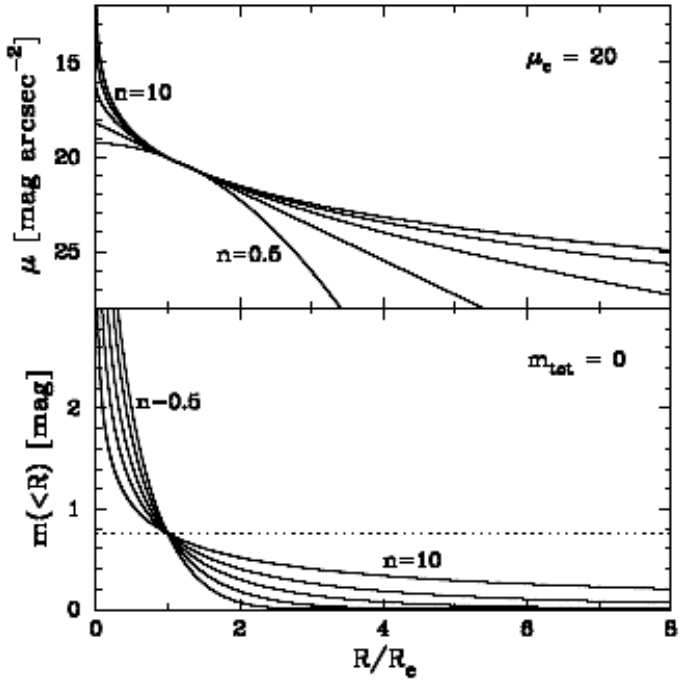

Figure 1: Top panel: Sérsic surface brightness profiles (Equation 6) for n=0.5, 1, 2, 4, and 10. The profiles have been normalised at $\mu_e = 20$ mag arcsec^{-2}. Bottom panel: Sérsic aperture magnitude profiles (Equation 5), normalised such that the total magnitude equals zero. The dotted line is offset by 0.75 mag (a factor of 2 in flux) from the total magnitude.

Graham & Driver 2005

Hubble sequence and color distribution
ハッブル分類とカラー分布

- Early-type galaxies have systematically redder colors than late-type galaxies.

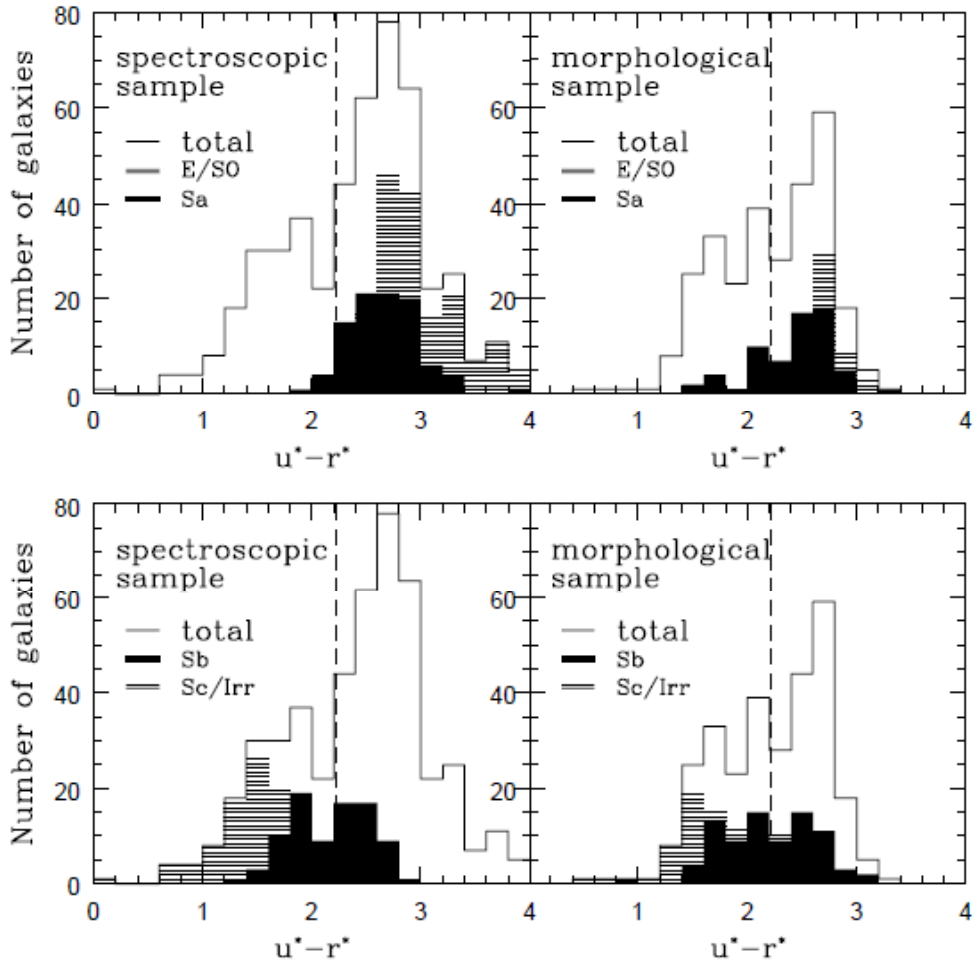

FIG. 7.—*Left*, Spectroscopic classification and u^*-r^* color; *right*, morphological classification and u^*-r^* color; *top*, histograms of early-type galaxies (E/S0 or Sa); *bottom*, those for late types (Sb or Sc/Irr).

Strateva et al. 2001, AJ, 122, 1861

Hubble sequence and physical properties I
ハッブル系列と物理パラメータ I

- Physical properties of galaxies systematically vary along the Hubble sequence.

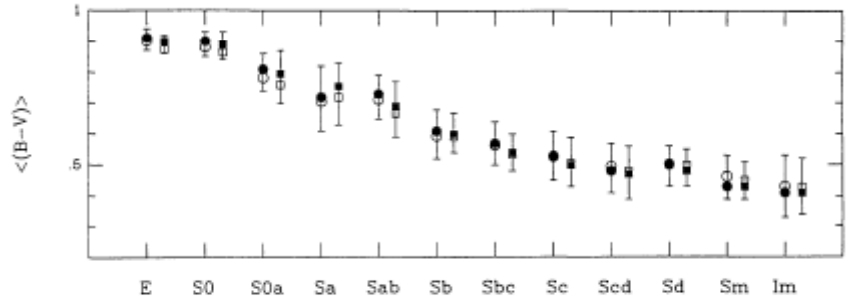

Figure 5 (B − V) color vs morphological type. (Same symbols as in Figure 2.)

Total mass determined with rotation curves of galaxies.

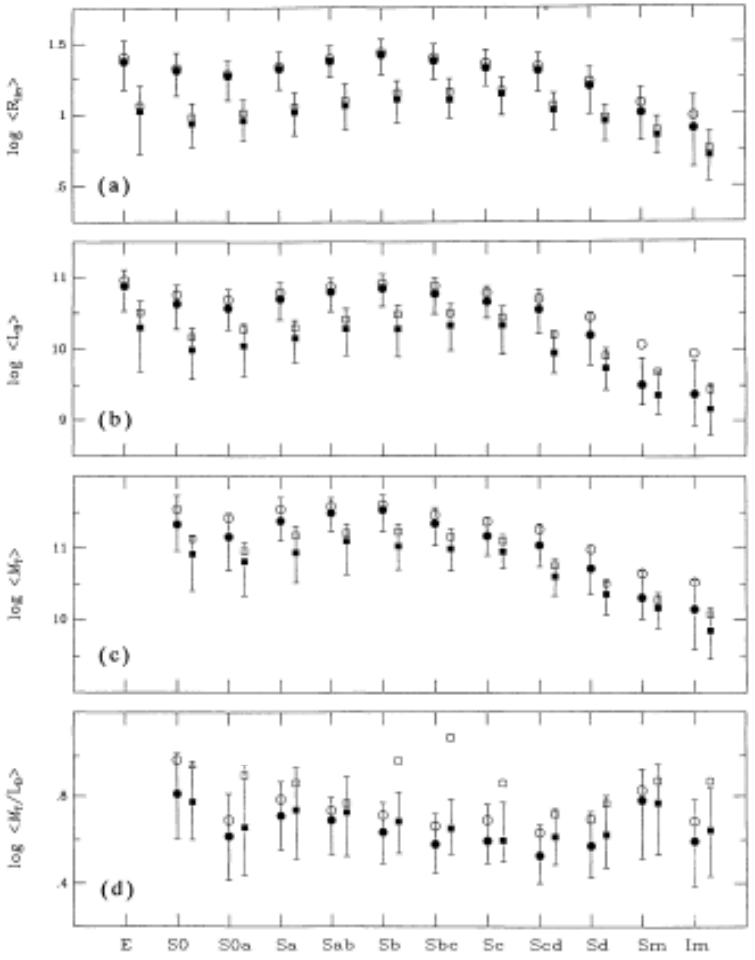

Figure 2 Global galaxy parameters vs morphological type. Circles represent the RC3-UGC sample; squares the RC3-LSc sample. Filled symbols are medians; open ones are mean values. The lower bar is the 25th percentile; the upper the 75th percentile. Their range measures half the sample. The sample size is given in Table 1. (*a*) log linear radius R_{25}(kpc) to an isophote of 25 B mag/arcsec^2 , (*b*) log blue luminosity L_B in solar units, (*c*) log total mass M_T in solar units, (*d*) log total mass-to-luminosity ratio M_T/L_B.

Roberts & Haynes, 1994, ARAA, 32, 115

Hubble sequence and physical properties II
ハッブル系列と物理パラメータ　II

- Physical properties of galaxies systematically vary along the Hubble sequence.

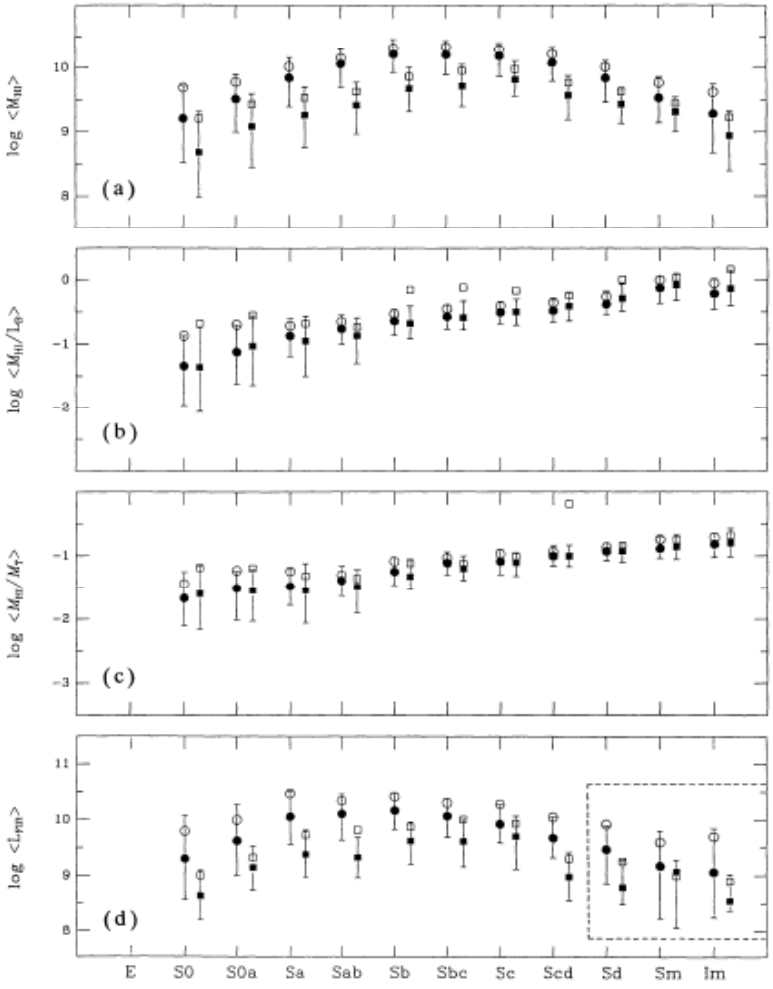

Figure 4 Same as Figure 2, for (*a*) log total HI mass M_{HI}, (*b*) log HI mass-to-blue luminosity ratio M_{HI}/L_B, (*c*) log HI mass fraction M_{HI}/M_T, (*d*) log FIR luminosity L_{FIR}. The dashed lines indicate significantly fewer data for these types.

Roberts & Haynes, 1994, ARAA, 32, 115

Galaxy “luminosity function” by galaxy type
銀河のタイプ別の光度関数

- Galaxy L.F. by ~1,500 galaxies from SDSS. Bright-end of the LF is dominated by E/S0 galaxies. Irr galaxies only appear in faint-end of the LF. Classification is also done with concentration parameter C=r50/r90.

TABLE 1
MORPHOLOGICALLY CLASSIFIED SAMPLE

Sample	$0 \le T \le 1$ (E and S0)	$1 < T \le 3$ (S0/a–Sb)	$3 < T \le 5$ (Sbc–Sd)	$5 < T \le 6$ (Im)	$T = -1$ (Unclass.)	Total
1. Photometric sample	740	630	444	35	26	1875
2. Spectroscopic sample	630	545	381	23	21	1600
3. Sample with good photometry	617	539	373	21	12	1562
4. Sample with z (≥85% CL)	616	538	369	19	11	1553
5. Sample used in MDLF	597	518	350	(10)	(7)	1482
6. Sample used to obtain ϕ^*	314	368	253	(5)	...	894

Nakamura et al. 2003, ApJ, 125, 1682

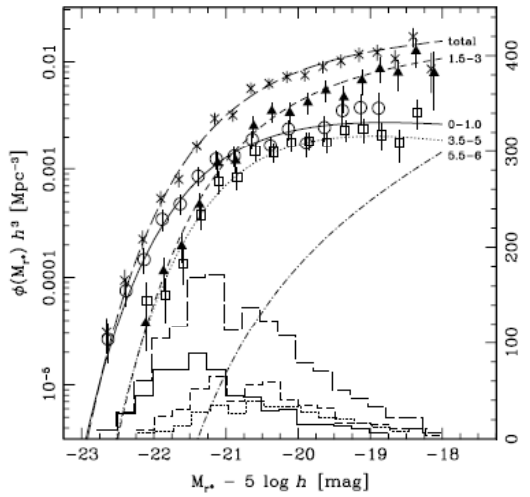

FIG. 3.—MDLF in the r^* band for three types, E–S0, S0a–Sb, and Sbc–Sd, from visual classifications. The SWML results are represented by data points (*circles*, E–S0; *triangles*, early spiral galaxies; *squares*, late-type spiral galaxies), and the ML fits are shown by solid, short-dashed, and dotted curves, respectively. The ML estimate for Im galaxies is represented by the dot-dashed curve. The luminosity function for the total sample is also plotted for comparison, represented by crosses and the long-dashed curve. The histograms are the actual numbers of galaxies for the three types and the total sample used in this analysis.

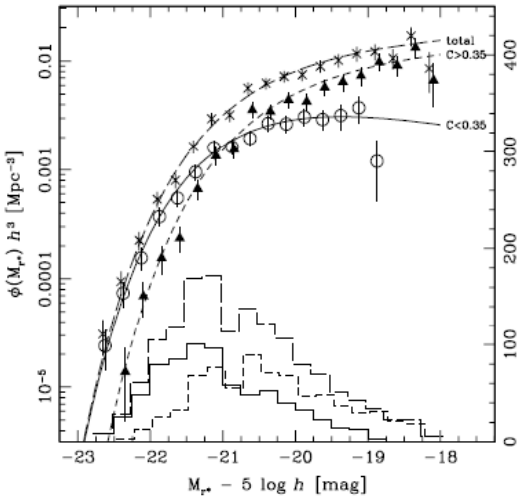

FIG. 6.—MDLF for early- and late-type galaxies classified using the concentration index. The SWML results are represented by data points (*circles*, early-type, with $C < 0.35$; *triangles*, late-type, $C > 0.35$), and the ML fits are shown by solid and short-dashed curves, respectively. The luminosity function for the total sample is plotted for comparison, represented by crosses and the long-dashed curve. The histograms are the numbers of galaxies used in this analysis.

Galaxy “luminosity function” by galaxy type
銀河のタイプ別の光度関数

- Luminosity function determined with the K-band photometry.

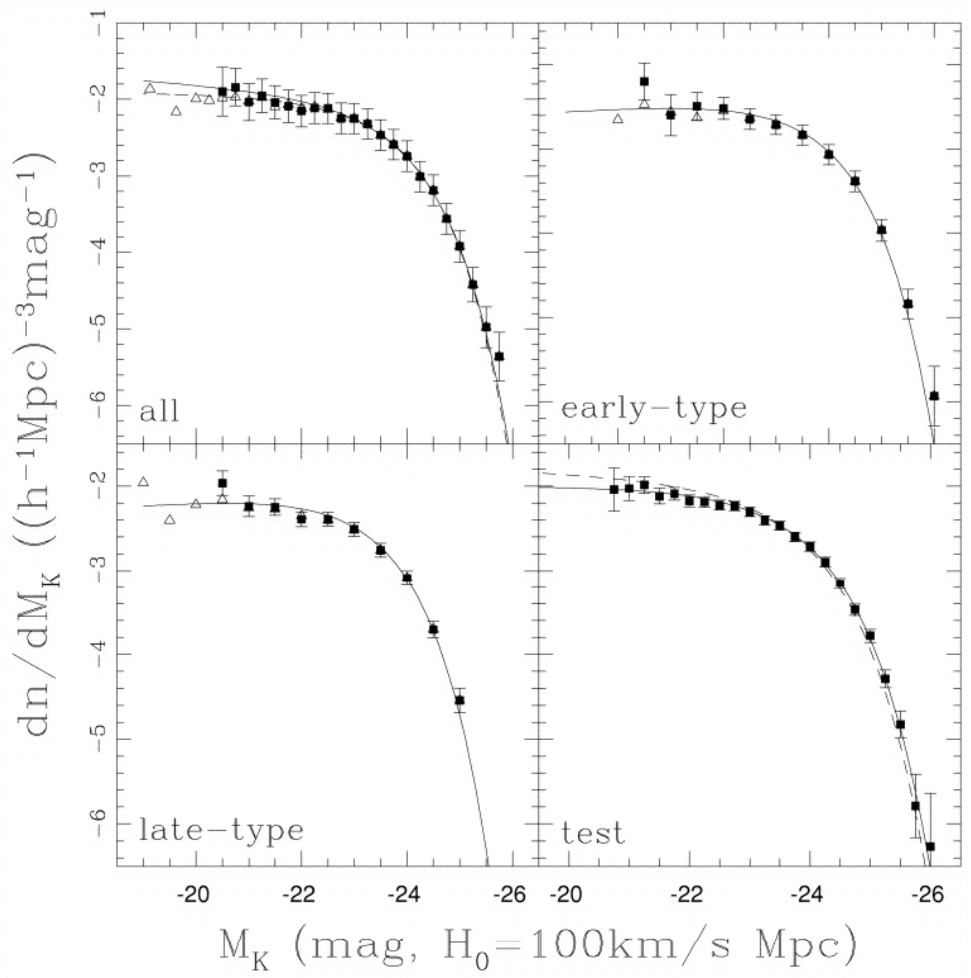

Kochanek et al. 2001, ApJ, 560, 566

Galaxy (stellar) “mass function by galaxy type
銀河のタイプ別の(星)質量関数

- Determined with SDSS+2MASS database

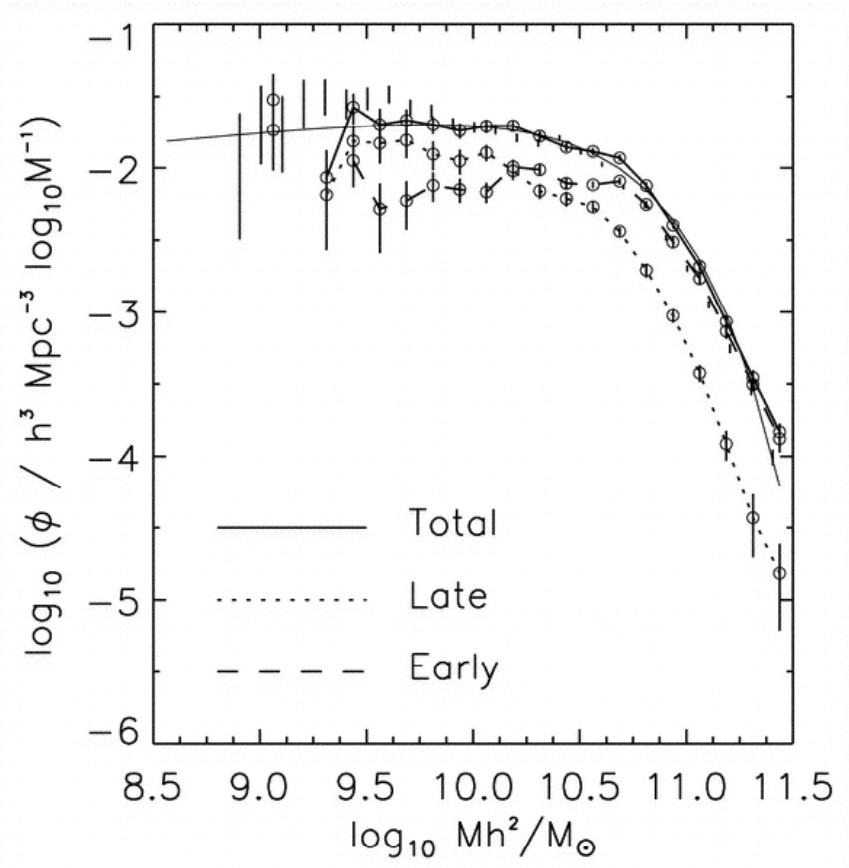

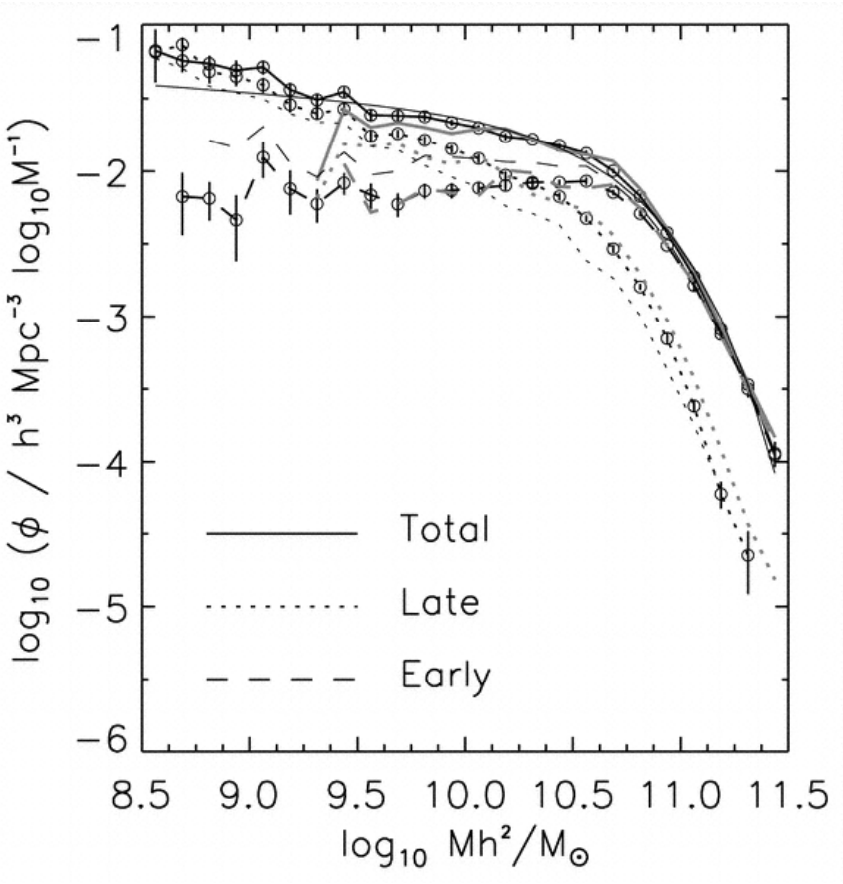

Bell et al. 2003, ApJS, 149, 289

Barred galaxies
棒状銀河

- Early-type barred galaxies sometimes show ring-like structure due to the orbital resonance (共鳴).

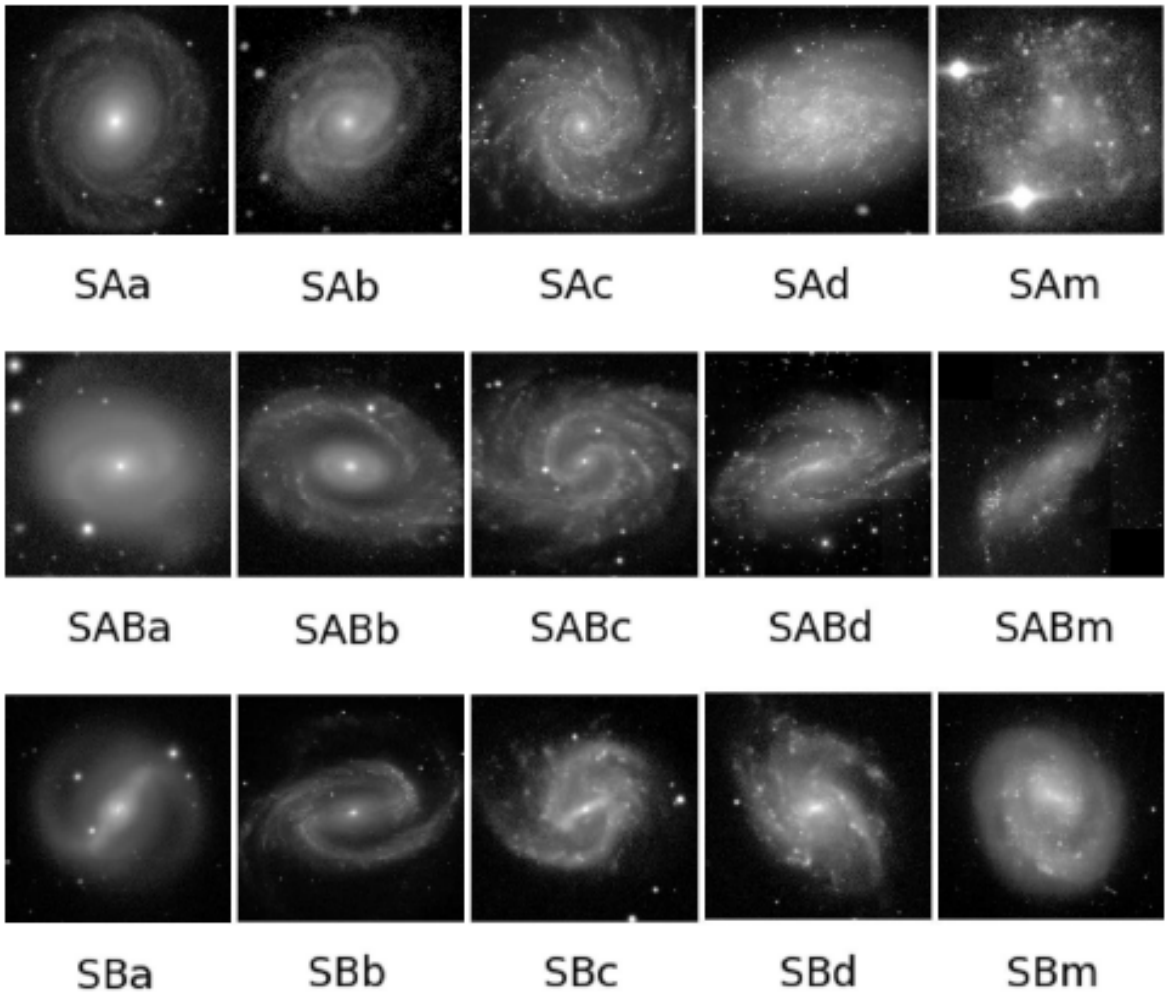

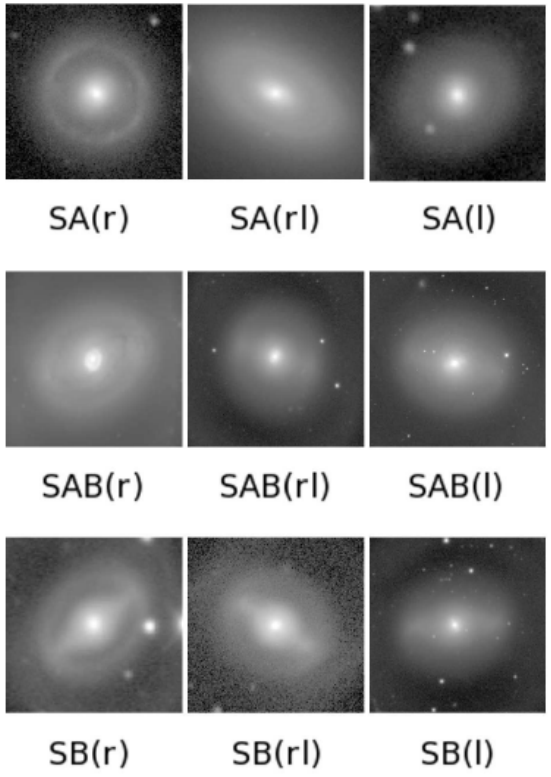

Buta, 2011, arXiv:1102.0550

Fraction of barred galaxies
棒状銀河の割合

- They are not minority among the spiral galaxies

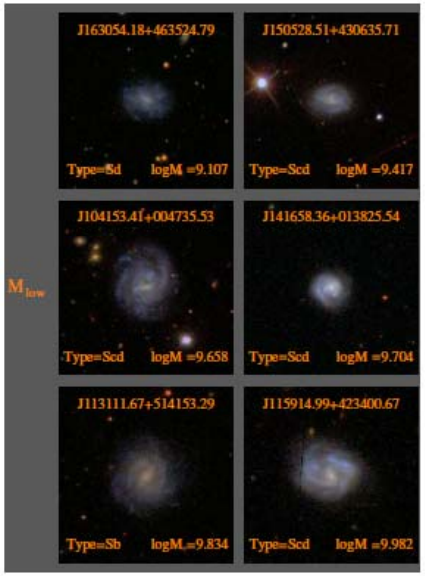

Figure 2. Two columns show a random sample of bars below the transition mass of 10.2. The J2000 object identifier is listed at the top, the type in the bottom left corner, and the mass on the right. Objects are arranged in order of increasing mass.

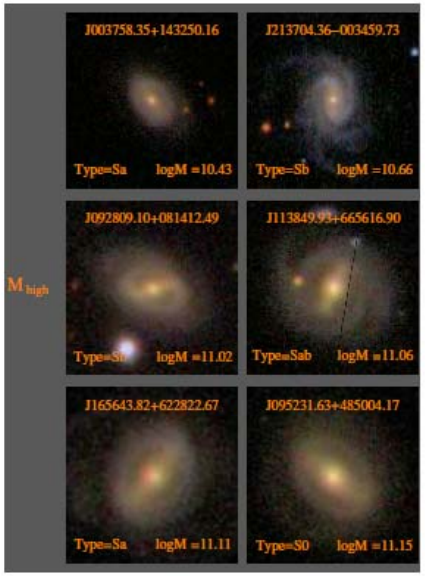

Figure 3. Two columns show a random sample of bars above the transition mass of 10.2. The J2000 object identifier is listed at the top, the type in the bottom left corner, and the mass on the right. Objects are arranged in order of increasing mass.

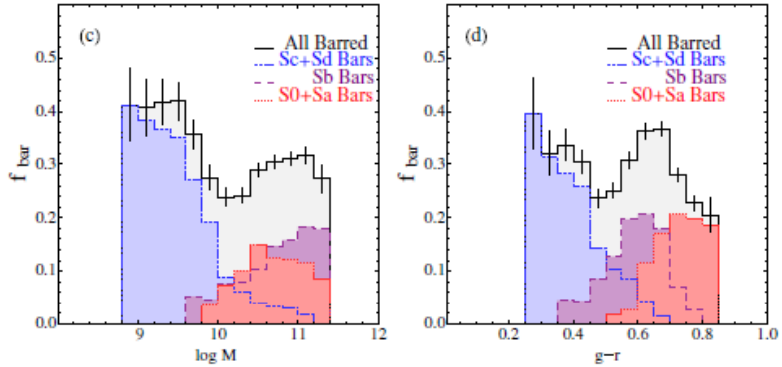

Nair & Abraham, 2010, ApJL, 714, L260

Figure 1. Top: histograms and fractional distribution of (a/c) stellar mass as defined by Kauffmann et al. (2003a) and (b/d) $(g-r)$ color for barred galaxies. The distribution of bars in S0+Sa (red), Sb (purple), and Sc+Sd (blue) galaxies as well as all barred galaxies (black) are shown. We find that the bar fraction falls steeply from low masses to intermediate masses, $M \sim 10.2$, and rises slowly and plateaus thereafter. With $(g-r)$ color, we find that the bar fraction decreases from bluer colors to intermediate colors, $(g-r) \sim 0.5$, and rises slowly thereafter.

Fraction of Barred galaxies
棒状銀河の割合

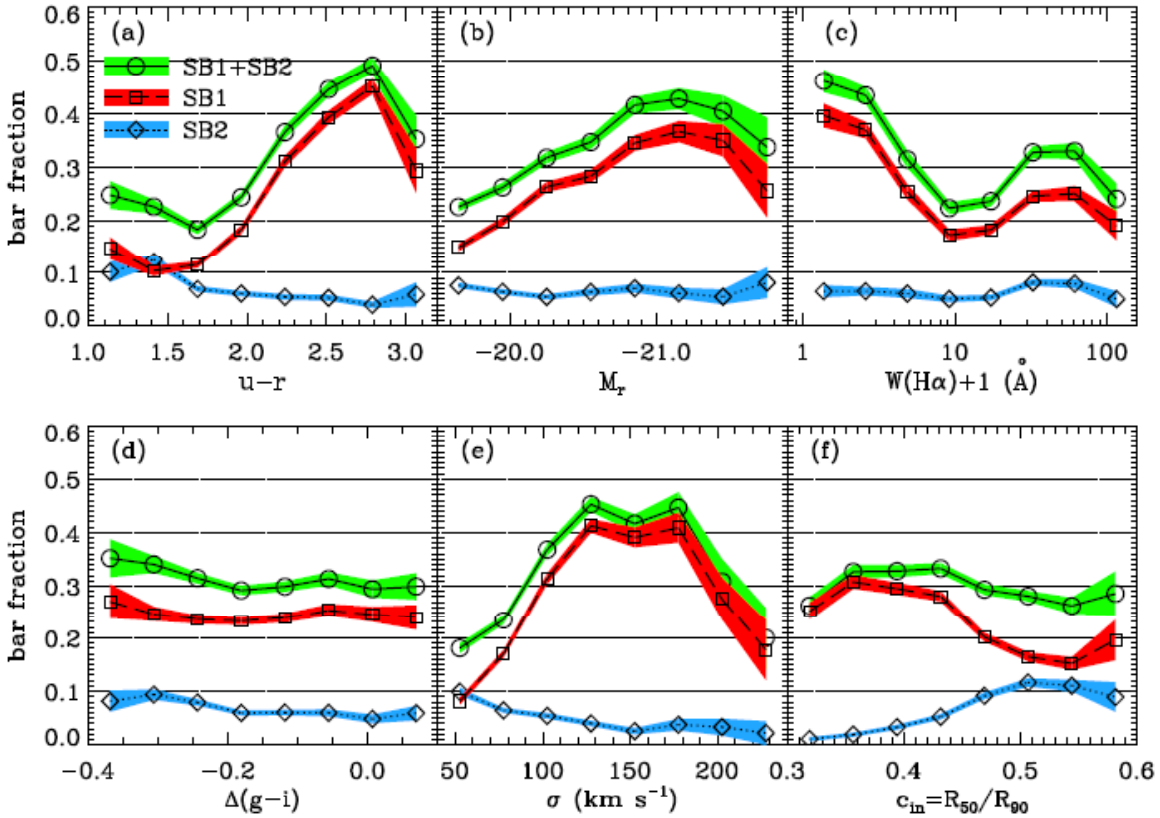

FIG. 7.— Dependence of the bar fraction for late-type galaxies on (a) $u-r$ color, (b) r-band absolute magnitude, (c) equivalent width of the $H\alpha$ line, (d) color gradient, (e) central velocity dispersion, and (f) inverse concentration index. Squares and diamonds represent, respectively, fraction of SB1 (strong bar) and SB2 (weak bar) galaxies. Circles represent the sum of both types. Shades mean 1-σ sampling errors.

SB1: Strong bar

SB2: Weak bar

Lee et al. 2011, arXiv:1110.1933

Cosmological evolution of the bar fraction
棒状銀河の割合の宇宙論的進化

- Fraction of barred spiral galaxies (bar-fraction) shows rapid increase between z=1 and 0.
- The increase is more rapid for galaxies with smaller stellar mass.

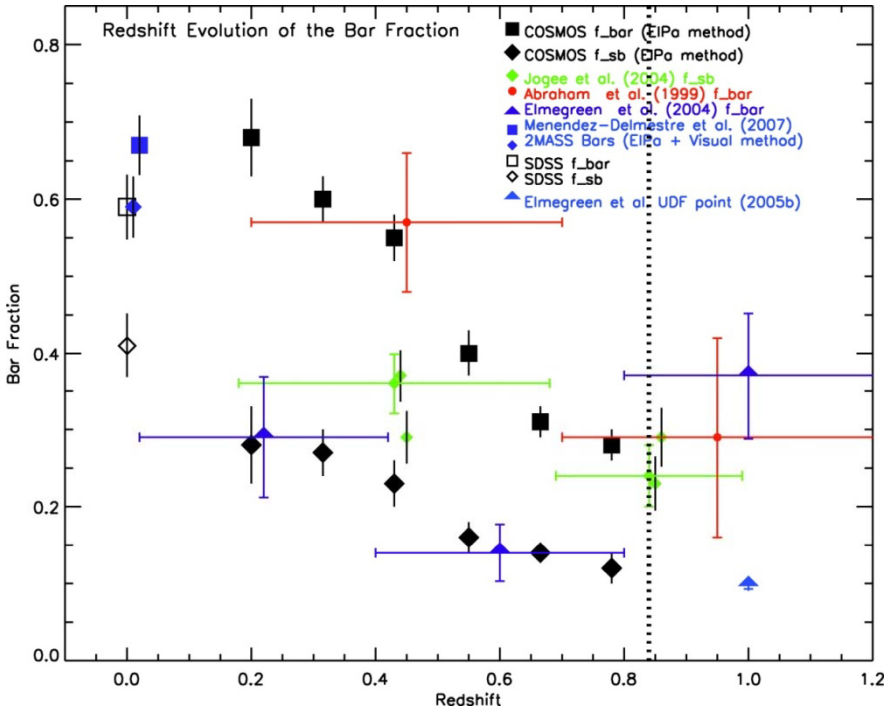

Sheth et al. (2008, ApJ, 675, 1141)

Based on COSMOS HSC dataset

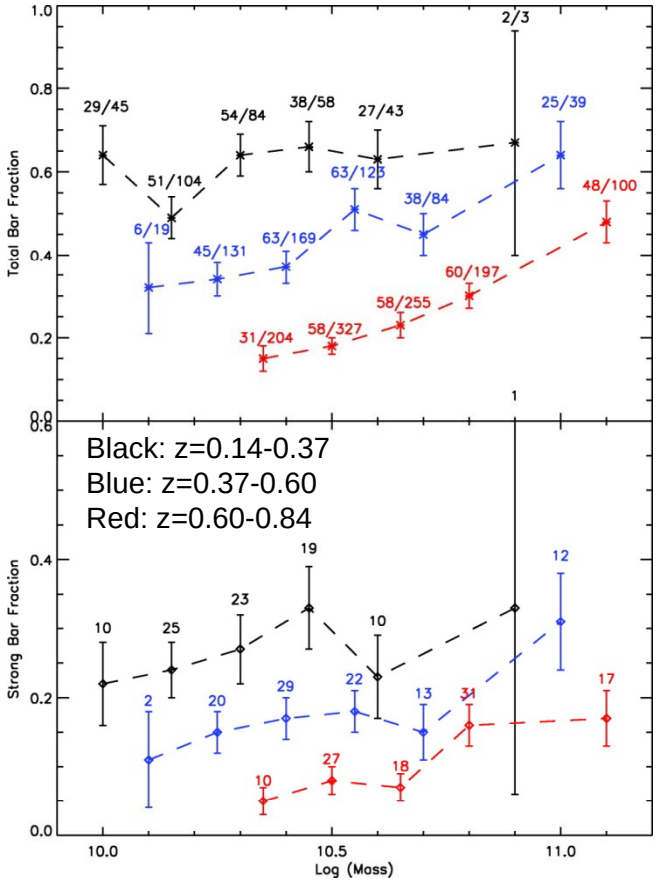

What does determine the observed relation between SMBH mass and "spheroid" mass ?

What are the spheroid ?

Sersic index of E/S0 “spheroids”
E/S0 のセルシックインデックス

- Best fit sersic index for E/S0 galaxies depends on effective radius and absolute magnitude.

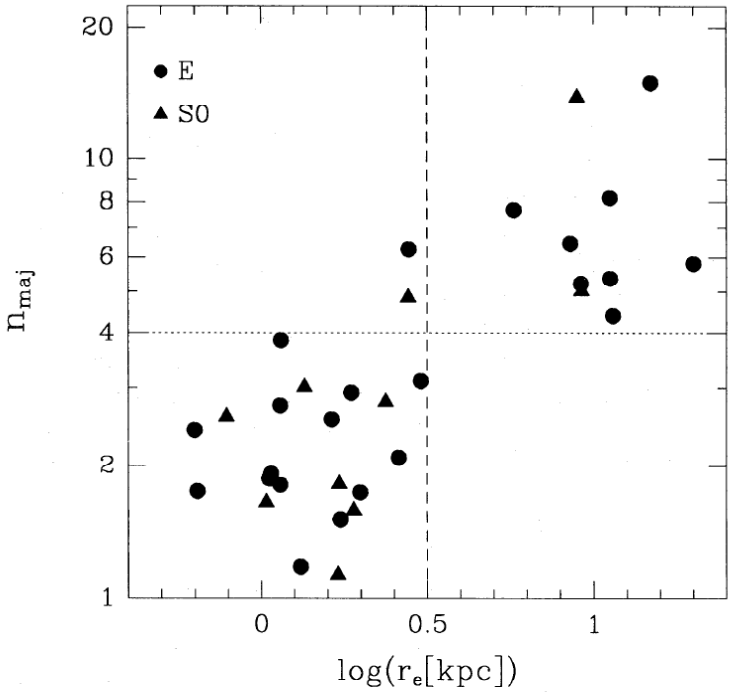

Figure 3. Plot of n_{maj} versus the effective radius $\log r_e$ (kpc) for the galaxies of our sample. Circles are for ellipticals and triangles for S0s. The dotted line marks the value $n = 4$, corresponding to the de Vaucouleurs law; the dashed line ($r_e = 3$ kpc) marks the separation between the 'ordinary' and 'bright' galaxy families.

Caon et al. 1993,

MNRAS, 265, 1013

Bulge and pseudo-bulge
バルジと「疑似」バルジ

- Bulge-like structures of late-type disk galaxies can be fitted with low Sersic index profile ~1, i.e. exponential-law. Such bulges are called psuedo-bulge.

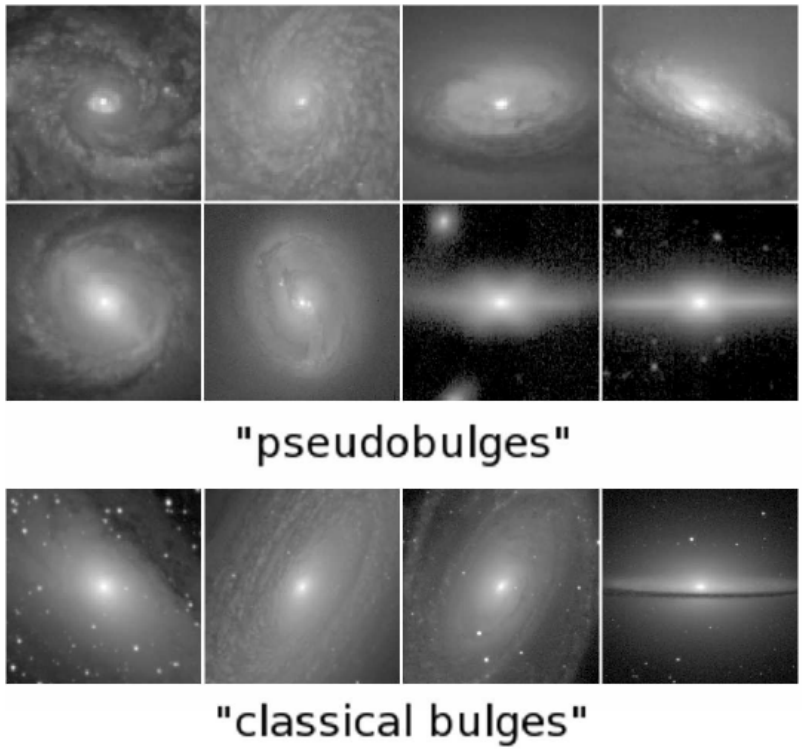

Buta, 2011, arXiv:1102.0550

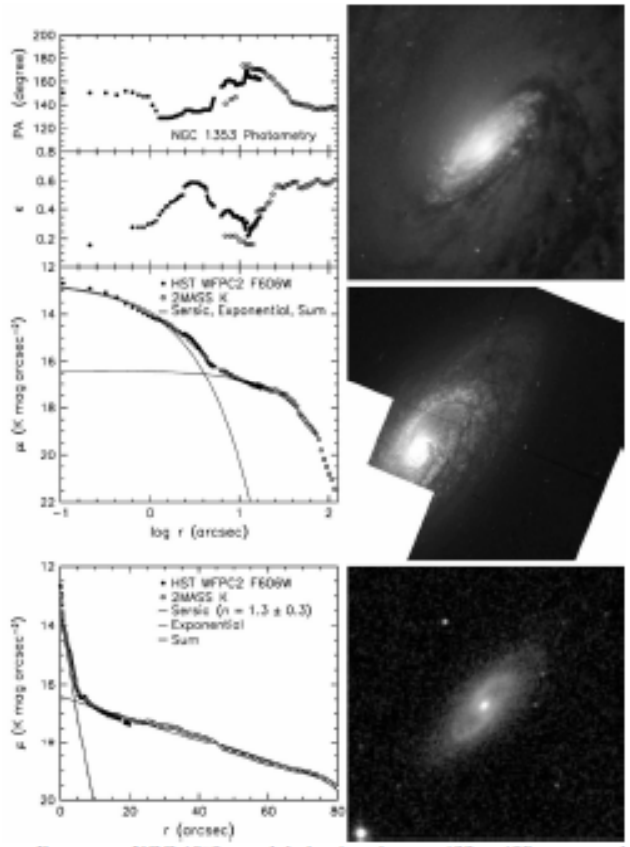

Figure 10 NGC 1353 pseudobulge (top image: 18″ × 18″ zoom, and middle: full WFPC2 F606W image taken with *HST* by Carollo et al. 1998). The bottom panel is a 2MASS (Jarrett et al. 2003) *JHK* composite image with a field of view of 4′.4 × 4′.4. The plots show surface photometry with the *HST* profile shifted to the *K*-band zeropoint. The lines show a decomposition of the major-axis profile into a Sérsic (1968) function and an exponential disk. The outer part of the pseudobulge has the same apparent flattening as the disk. This nuclear disk produces much of the rapid upturn in surface brightness toward the center.

Kormendy 2004, ARAA, 42, 603

Lack of n~4 galaxies at high redshifts ?
高赤方偏移では n~4 がほとんどいない？

- Adaptive Optics observations of z~3 galaxies (11Gyrs ago) reveals lack of galaxies with n~>4.

Akiyama et al. 2008, ApJS, 175, 1